Downloaded from orbit.dtu.dk on: Apr 25, 2025

DTU Library

High-Throughput Wafer-Scale Wrinkle Patterning
A Single-Step Fabrication Process and Applications for Tunable Optical Transmittance

Chang, Bingdong; Zhao, Ding; Sun, Hongyu

Published in:
ACS Applied Electronic Materials

Link to article, DOI:
10.1021/acsaelm.1c00380

Publication date:
2021

Document Version
Peer reviewed version

Link back to DTU Orbit

Citation (APA):
Chang, B., Zhao, D., & Sun, H. (2021). High-Throughput Wafer-Scale Wrinkle Patterning: A Single-Step Fabrication Process and Applications for Tunable Optical Transmittance. *ACS Applied Electronic Materials*, *3*(7), 3200-3206. https://doi.org/10.1021/acsaelm.1c00380

General rights
Copyright and moral rights for the publications made accessible in the public portal are retained by the authors and/or other copyright owners and it is a condition of accessing publications that users recognise and abide by the legal requirements associated with these rights.

- Users may download and print one copy of any publication from the public portal for the purpose of private study or research.
- You may not further distribute the material or use it for any profit-making activity or commercial gain
- You may freely distribute the URL identifying the publication in the public portal

If you believe that this document breaches copyright please contact us providing details, and we will remove access to the work immediately and investigate your claim.

High-throughput wafer-scale wrinkle patterning: a single-step fabrication process and applications for tunable optical transmittance

Bingdong Chang [1], Ding Zhao [2], Hongyu Sun [3]

1. DTU Nanolab, Technical University of Denmark, Ørsteds Plads, Building 347, 2800 Kgs. Lyngby, Denmark.

2. Key Laboratory of 3D Micro/Nano Fabrication and Characterization of Zhejiang Province, School of Engineering, Westlake University, 18 Shilongshan Road, Hangzhou, 310024 Zhejiang Province, China

3. DENSsolutions B. V., Informaticalaan 12, 2628 ZD Delft, Holland

KEYWORDS: wrinkles, random gratings, smart window, tunable optical transmittance, plasma treatment

ABSTRACT

The engineering of wrinkled surfaces has attracted enormous research interests, especially for optical applications. However, the standard fabrication processes rely on the routine with skin layer generations and controlled mechanical deformations, which are normally performed separately with dedicated equipment, limiting the possibility for large-scale practical applications. In this work, we have developed an effective fabrication strategy to pattern wafer-scale wrinkles on photoresists. By performing a fluorine-based plasma treatment, skin layers can be generated and thermal stress is induced simultaneously, due to the limited heat dissipation from substrates. Uniform wrinkling across the wafer is achieved with few seconds of plasma processing, and the morphology of wrinkles has been investigated in terms of the photoresist thickness, ion energies and process times. The wrinkled resists can be transferred into silica substrates for quasi-random SiO_2 gratings, leading to tunable optical transmittances depending on the filling ratio. An application for reversible optical transmittance is also demonstrated, when organic solvents is applied to reduce the scattering losses on the grating surfaces. We believe our technique can pave the way towards high-throughput CMOS-compatible fabrications of wrinkle-based devices, which can be interesting for various fields due to the unique quasi-random surface morphology.

INTRODUCTION

Spontaneous generation of wrinkles has become a versatile and cost-efficient technique for surface patterning and engineering in the last few decades. By exploiting the wrinkled surfaces, which are normally on a mechanically flexible substrate, various applications have been demonstrated to tailor the optical responses, [1, 2] mechanical properties [3, 4] and electronic performances. [5] Specifically, the wrinkled surface structures can act as diffusers to reduce the optical transmittance in a broad spectrum, making it possible to fabricate smart windows with tunable optical transmittances. [6 - 8] The wrinkle generation is a dynamic process and depends on the unparalleled Young's modulus of the skin layer and the substrate. [9, 10] There are two crucial steps for controllable wrinkling processes: skin layer generation and mechanical deformation. In conventional studies, these two steps are performed separately and thus dedicated experimental equipment is required sequentially. The skin layer can normally be generated by depositing additional materials, [11, 12] ultraviolet-ozonolysis (UVO) treatments, [13, 14] plasma process, [15, 16] etc, while the mechanical deformation can be achieved with axial stretching, [12, 16] solvent induced swelling, [13, 14] thermal treatment, [11, 15] etc. These processes are sometimes time consuming and limiting the possibilities for large-scale production. Besides, the wrinkled structures are mostly limited in polymer materials like polydimethylsiloxane (PDMS) and polystyrene (PS), which require specialized treatment techniques that are not standard in CMOS industries.

Here we present a novel technique to generate wrinkled patterns on a wafer scale by combining the two steps into a single-step process. The wrinkles are fabricated with commercially available photoresist with wafer substrates. While the skin layer is generated by plasma treatments, a thermal

stress is introduced simultaneously by the plasma-induced heating, thus wrinkles can be generated inside a single instrument within few seconds. The fabricated wrinkles have a good uniformity in both wavelengths and amplitudes, which can be modified by tuning ion energies and process time. The wrinkles can be transferred conveniently into a fused silica substrate, giving silicon dioxide (SiO_2) quasi-random gratings which can act as optical diffusers, thus the optical transmittance can be tuned continuously by controlling the process time when the wrinkles are transferred by plasma etching. The quasi-random SiO_2 gratings can be infiltrated by solvent and dried by nitrogen gas (N_2) conveniently, enabling a reversible transformation between optically translucent and opaque states. We believe this approach can reduce the fabrication difficulty significantly for large area wrinkle patterning, thus benefiting the study and production of wrinkle-based devices.

RESULTS AND CONCLUSIONS

Figure 1a shows the process flow schematically. Firstly, the whole wafer is coated by photoresists with an initial thickness of t_R. Afterwards, the resist-coated wafer is placed on top of a carrier wafer without any adhesives (the center area of the carrier wafer is etched by around 100 µm to fix the sample), and a fluorine-based plasma treatment is then performed with hexafluoride gases (SF_6). While the carrier wafer is clamped electrostatically on the platen electrode with helium backside cooling, the heat transfer between the carrier and the resist-coated wafer is limited, since it merely relies on thermal radiations between a vacuum gap, and the heat induced by plasma treatment can be then confined inside the resist-coated substrate. Depending on the ion energy and ion density, the temperature on the substrate (*T*) can exceed the glass transition temperature of the photoresist (T_g). For most of the photoresists T_g is below 150 °C, [17] and the substrate temperature

T can reach beyond 160 °C or even higher during a plasma process. [18] In the same time, the fluorine-based plasma can generate a stiff skin layer on the surface of photoresists, which has a higher Young's modulus compared with the bulk photoresist beyond T_g, [16] thus wrinkles can be generated on a whole wafer scale due to the thermal stress. It has been reported before that the fluorine-based plasma can fluorinate the carbon backbone on polymer surfaces.[19] The plasma treatment takes only few seconds, which is significantly faster compared with conventional techniques for wrinkle generations. In our study, wafer-scale wrinkles have been successfully produced by using two types of commercially available photoresists, AZ MiR 701 and AZ 5214E (Microchemicals GmbH), which is demonstrate by the photographic images in Figure 1b, and the corresponding surface morphologies are also presented by atomic force microscopic (AFM) images. The wrinkles on AZ MiR 701 are characterized by AFM on a range of 8 cm as shown in Figure 1c, the average wavelength λ is measured to be 2.995 μm and the average amplitude A is 396 nm, with a deviation of 5.3% and 5.8% correspondingly. It should be addressed that the good uniformity of wrinkles is enabled by the plasma etching system being used, which is able to generate high density plasma uniformly on a substrate with the size up to 6-inch. For the wrinkles of a thin skin layer on top of a shallow substrate, the wrinkle wavelength λ is given by $\lambda \sim (t_S t_R)^{1/2} (E_S/E_R)^{1/6}$, while the amplitude A can be described as $A \sim (\Delta/W)^{1/2} \lambda$, [9] here t_S is the thickness of the skin layer, and E_S and E_R are the Young's modulus for the skin layer and the resist correspondingly, Δ is the imposed compressive displacement and W is the width of resist covered area (in this case the width of the wafer). For various t_R from 770 nm to 1482 nm, the AFM-scanned wrinkled surfaces are presented in Figure 1d and Figure 1e, where the wrinkles exhibit a sinusoidal profile (scanning electron microscopic images (SEM) images are shown in Figure S1). The measured λ and A are plotted in Figure 1f, showing positive correlations with an increasing t_R

, which agrees with the classical wrinkle theories (here the samples have been processed with same plasma conditions, thus t_S is considered to be the same. A detailed data fitting from the experimental results suggest some higher order terms in the correlation between λ and t_R, which doesn't totally agree with the classical wrinkle models, this however is beyond the discussions in this work).

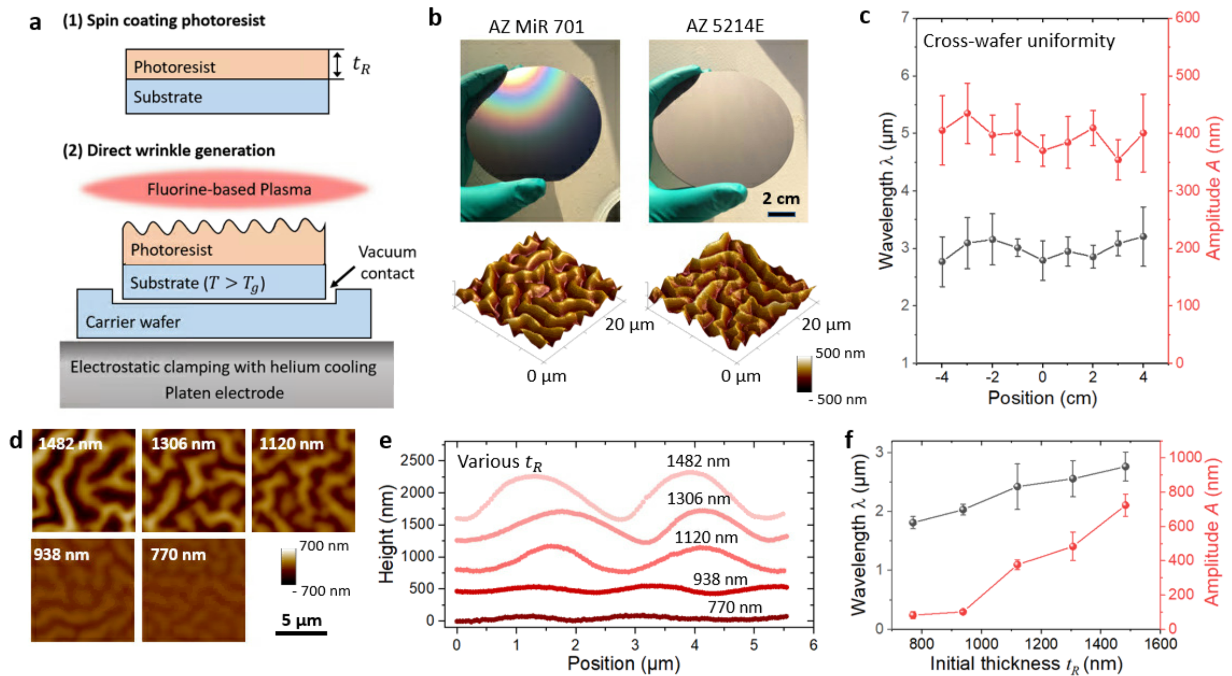

Figure 1. (a) Process flow for large-scale wrinkle patterning on photoresists; (b) photographic images of wrinkles on whole 4-inch wafers and corresponding AFM-scanned surface profiles, two types of photoresist (AZ MiR 701 and AZ 5214E) are being used; (c) cross-wafer uniformity of wrinkle patterns (AZ MiR 701) with regard to wrinkle wavelengths and amplitudes; (d) AFM-scanned surface profiles for wrinkles with different initial thicknesses of photoresists (AZ MiR 701), the wrinkle wavelengths and amplitudes are compared in (e) and (f), notice that the surface profiles for various thicknesses in (e) are shifted by 500 nm for clarity.

While the skin layer generation during plasma processing has been widely investigated, [16, 20] the essence of this technique is to exploit the simultaneous heat generation during the plasma treatment. In order to maximize the available plasma energy to be transferred into thermal energies inside the substrate, a balance should be achieved between the density and the kinetic energy of ions. Generally, a higher pressure can increase the ion density in a certain range with a specified power on the coil electrode, however this will limit the kinetic energy of ion bombardments. [21, 22] Here we chose pressure of 20 mTorr and the ion energy is tuned by varying the power supply on the platen electrode, the ion energy is then estimated by measuring the bias voltage combined with the self-bias potential (around -25 V). **Figure 2a1** and Figure 2b1 present the AFM-scanned wrinkled surfaces on AZ MiR 701 and AZ 5214E (t_R ~ 1.5 μm), when the ion energy varies between ~100 eV and ~ 300 eV. While the wavelength of the wrinkles increases slightly for a higher ion energy, a significantly larger wrinkle amplitude can be achieved with maximized ion energy, which is shown in Figure 2a3 and Figure 2b3. This positive dependence of λ and A on the ion energy is understandable, since a larger penetration depth of ions can be achieved with a higher bias potential, therefore the skin thickness t_S increases, besides, a larger Young's modulus E_S has also been reported before for higher ion energies. [20] As the heat dissipation from the sample substrate is limited with our setup, a longer process time can increase the stored thermal energy and thus a higher sample temperature, leading to an increased thermal stress-induced transverse displacement Δ. Besides, a larger skin thickness t_S has been demonstrated for longer plasma treatment before. [16] Thus when the time is varied from 5s to 12s for plasma processes, both kinds of photoresists exhibit increasing λ and A. It should be mentioned that degassing of photoresists can happen in a vacuum environment and high temperatures, where the solvent evaporates from the bulk resist substrate, this will create surface roughness and also modify the mechanical property

of the substrate. It also implies that for polymer-based substrate, hardening pretreatment can be necessary in order to apply this technique.

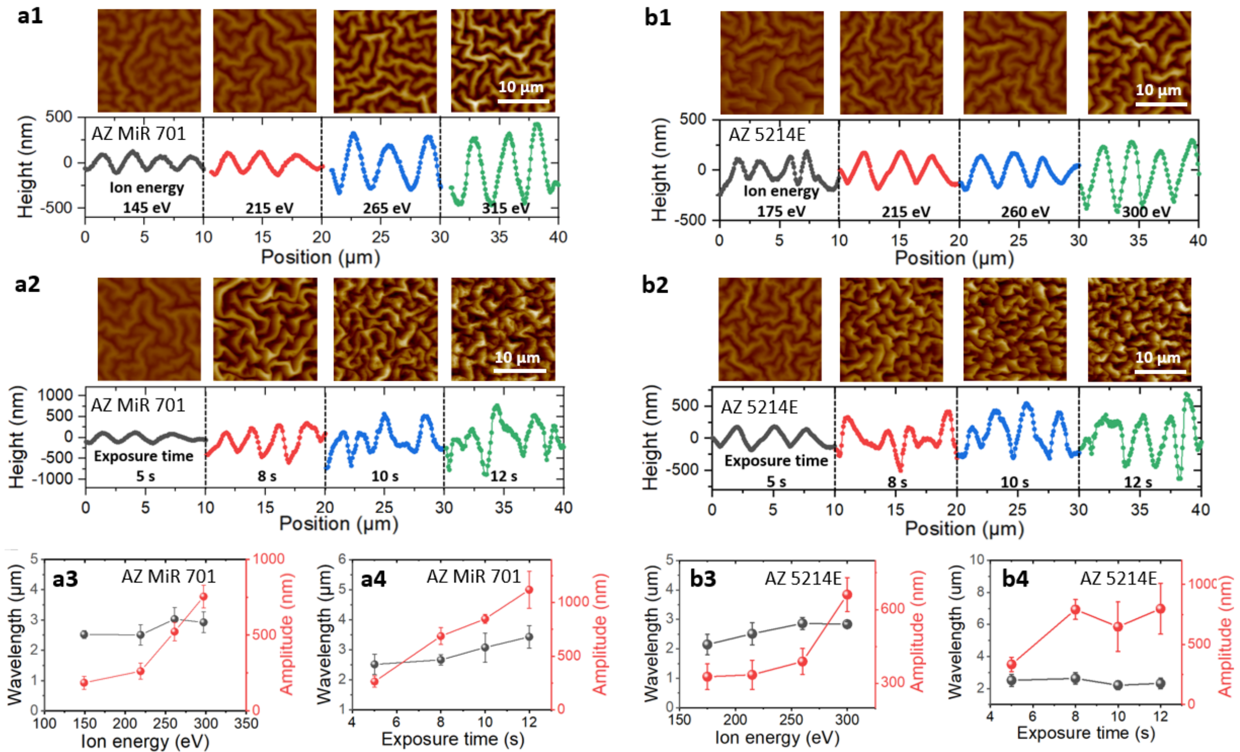

The plasma-induced heat generation can also be employed to pattern wrinkles on a thin metal film conveniently, and the process flow is illustrated in **Figure 3a**. A thin aluminum (Al) film with a thickness of t_M is deposited on photoresist layer (AZ MiR 701) by thermal evaporation, afterwards the sample is placed upside down on a carrier for plasma treatments. In this case the

ion bombardment will not directly influence the photoresist layer, instead the heat will be generated on the backside of substrate wafers and be conducted towards photoresists and the Al film. The Al film will hereby act as a skin layer and the wrinkles can be developed by 15 seconds of plasma processing. Compared with patterning wrinkles directly on photoresists, the thickness of Al film can be better controlled in term of thicknesses and film qualities. By choosing t_M as 50 nm, 100 nm and 150 nm, wavelengths and amplitudes of the wrinkles are compared as shown in Figure 3b. With an increasing t_M, λ increases almost linearly, while A is relatively stable, besides, a thicker resist (t_R = 1.5 μm) can increase both λ and A compare with t_R = 500 nm, which agrees with the classic wrinkle theories. AFM was applied to characterize the surface morphology of wrinkled Al film with t_M = 50 nm, and the typical sinusoidal waveforms can be observed (optical microscopic images are available in Figure S2). Here the roughness is caused by the grains of Al film deposited with thermal evaporations. By generating wrinkles in metal thin films assisted by plasma treatments, the flexibility of our technique is demonstrated, besides, the wrinkles in conductive materials are favorable for electric devices. [11]

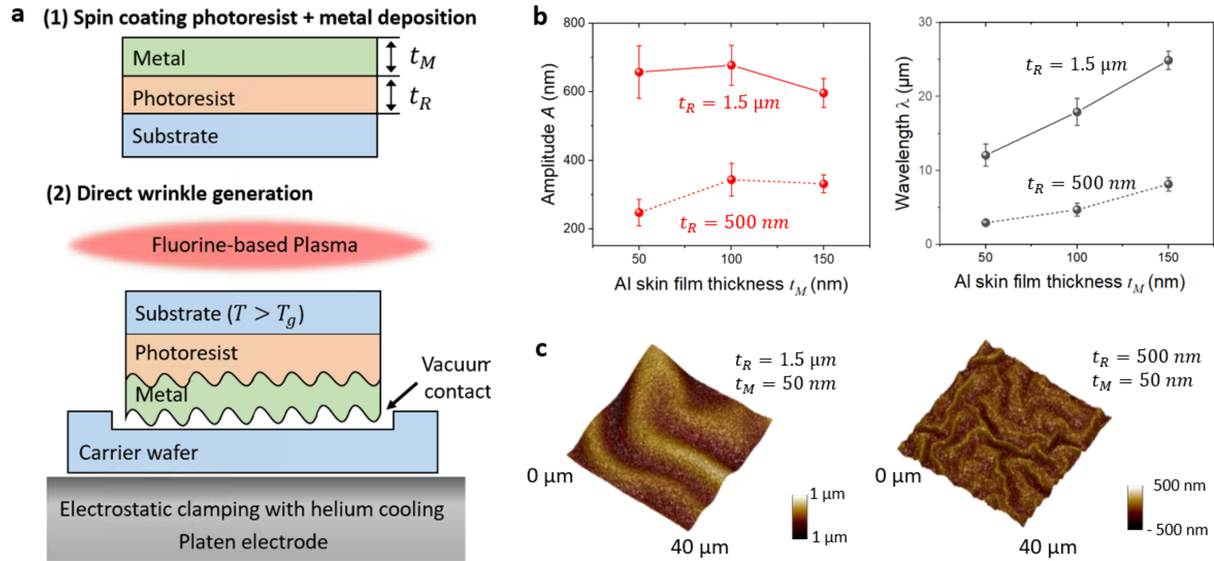

Figure 3. Generating wrinkles on a thin metal film to demonstrate the effect of plasma treatment: (a) illustration of the process flow, where the wrinkles are generated on thin metal films deposited on photoresist; (b) comparing the wavelength and amplitude of the wrinkles on Al films with various t_M, when the photoresist thickness t_R is set to be 1.5 μm and 500 nm; (c) AFM-scanned surface profiles with t_M = 50 nm and t_R of 1.5 μm and 500 nm.

Due to the refractive index contrast between the air and wrinkled materials, and the feature size of the wrinkles (typically larger than the visible wavelengths), the optical transmittance through the wrinkled substrate can be significantly reduced by the scattering losses. This property has been studied for wrinkles on PDMS films, which is optically transparent in visible wavelengths with a smooth surface. By applying mechanical stretching [7] or near-infrared irradiation on the wrinkled PDMS films, [11] wrinkles can be generated and erased irreversibly, enabling active modification of optical transmittance for smart window applications. In our study, the wrinkles are created on a thin photoresist layer, thus can be transferred directly into the rigid substrate with standard plasma etching equipment in semiconductor industries. Here we used fused silica as the substrate, which has a refractive index n_G ~ 1.46 at a wavelength of 500 nm, [23] and the wrinkles

are generated on AZ MiR 701 resist with t_R = 1.5 μm. **Figure 4a** shows schematically the evolution of structures, when wrinkled patterns are transferred into fused silica by a continuous plasma etching process. Due to the sinusoidal profile of the resist patterns, the distance between etched gratings will become larger ($D_2 > D_1$) with an increasing grating height ($H_2 > H_1$), when the plasma etching proceeds. Optical microscopic images (Figure 4b) present the morphology of the SiO_2 surfaces with increased plasma etching time (from top to bottom). It can be observed that the SiO_2 gratings inherited the quasi-random geometric feature from the photoresist wrinkles, and a longer plasma etching time will lead to a smaller filling ratio f (here f is defined by $f = 1 - D/\lambda$, with D as the distance between adjacent gratings). The broadband optical transmittance is measured on the quasi-random SiO_2 gratings as shown in Figure 4c. For $f = 1$ (bare fused silica substrate), the transmittance is over 0.9 on a broad spectrum range between 210 nm and 1690 nm. When f increases, the transmittance reduces on the whole measured spectrum, and a larger transmission loss is observed for smaller wavelengths. This is understandable, since the light propagation is less affected, when the optical wavelength is larger than the feature size on the quasi-random SiO_2 gratings. When f is close to 0, the grating structures are replaced by random surface roughness, giving a negligible transmittance close to 0 (a photographic image of a whole 4-inch fused silica wafer with quasi-random gratings on the surface is available in Figure S3).

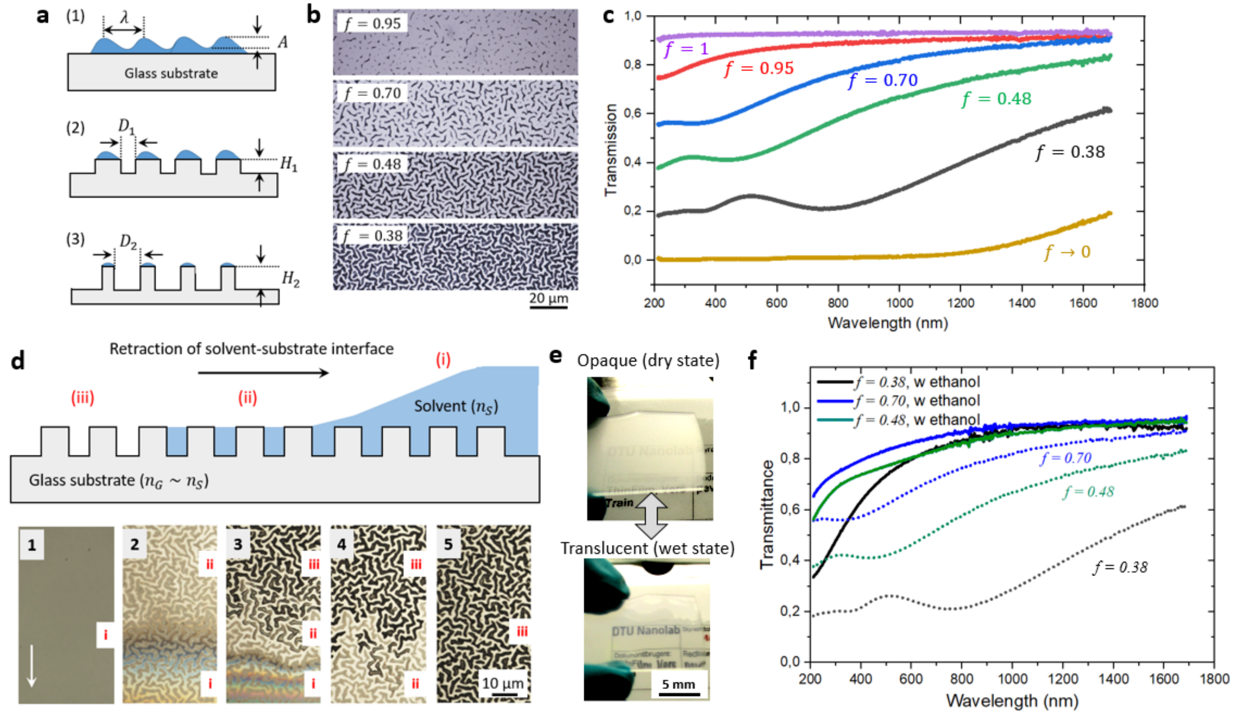

Figure 4. Tunable optical transmittance by transferring wrinkle patterns into SiO_2 substrates: (a) a schematic illustration showing the structure evolution, when wrinkle patterns are used as a mask to etch into SiO_2 substrate, forming grating structures; (b) optical microscopic images of quasi-random SiO_2 gratings with reduced filling factor f by increasing the etch time; (c) measured optical transmittances of quasi-random SiO_2 gratings with various filling factors between 0 and 1 (for f = 0, 0.38, 0.48, 0.7, 0.95 and 1, the total etch time is 20 min, 17 min, 15 min, 12 min, 10 min and 0 min correspondingly); (d) illustration of different stages (i, ii and iii) during solvent drying on top of the substrate, the process is demonstrated by optical microscopic images (from 1 to 5); (e) reversible transitions between the optically opaque state (without ethanol solutions) and the translucent state (ethanol solutions covering the whole sample surface); (f) Measured optical transmittances for quasi-random SiO_2 gratings with and without ethanol solutions coverage, improved transmittances are observed for three different filling factors.

In order to achieve a tunable optical transmittance, we infiltrated the quasi-random SiO_2 gratings with ethanol solutions, which has a refractive index n_S ~ 1.36 (at a wavelength of 500 nm) [24] and a relatively small surface tension of 22.31 mN/m. [25] When the ethanol solution is drop-casted on the substrate, the quasi-random gratings can be efficiently infiltrated due to the small surface tension, in the same time, the ethanol solutions will evaporate because of its relatively high vapor pressure. The infiltrating and evaporation process on the surface of SiO_2 gratings is illustrated in Figure 4d, where three different stages can be observed (which are also presented by optical microscopic images below): (i) the substrate is covered by ethanol; (ii) part of ethanol solutions is trapped between the gratings while the majority is evaporated; (iii) ethanol is fully evaporated leaving clean SiO_2 gratings. Since the refractive indexes of SiO_2 (n_G) and ethanol (n_S) is comparable (n_G~1.46 at a wavelength of 500 nm), the scattering loss on the grating surfaces can be reduced significantly when ethanol is applied, thus the optically opaque SiO_2 substrate can become translucent. This reversible process is demonstrated in Figure 4e, where the texts on the background can be observed visibly behind the SiO_2 sample, when ethanol is drop-casted on the surface. The transmittance spectra were acquired for samples with different f for the quasi-random gratings (Figure 4f), and the transmittance can be increased by up to 0.5 (f = 0.38, at a wavelength of 500 nm) with ethanol applied.

Compared with winkles on polymer-based materials, a rigid substrate can be favorable for applications like smart windows, especially in harsh environments (like large mechanical stress, high humidity, etc). However, the optically translucent and opaque states have to be durable for practical uses, thus the solvent has to be confined inside a cavity free from evaporations. To solve this issue, an optically transparent fused silica wafer was used as a cladding layer, which was bonded with the wafer with quasi-random gratings on surface (with a distance d ~ 500 μm, as

shown in **Figure 5a**). With this simple setup, ethanol solutions can be injected conveniently inside the cavity by a pipette, enabling an optically translucent state. For the opaque state, nitrogen gas was blown through the cavity and the ethanol could be expelled from the gratings. A demonstration of the setup based on a 4-inch wafer can be seen in Figure 5a, the transition between the translucent and opaque states takes around 2 seconds. As the ethanol is physically confined inside the channel between two wafers, the reduction of optical transmittances induced by solvent evaporations can be limited effectively, this is proved by the measured transmittance in Figure 5b, where the optical transmittance is reduced by around 20% after 5 hours (at a wavelength of 500 nm). In an ideal situation, the solvent can be circulating around the channels, thus the evaporation of solvents shouldn't be a problem practically. For a higher transmittance in the translucent state, solvents with a higher refractive index close to fused silica can be an option.

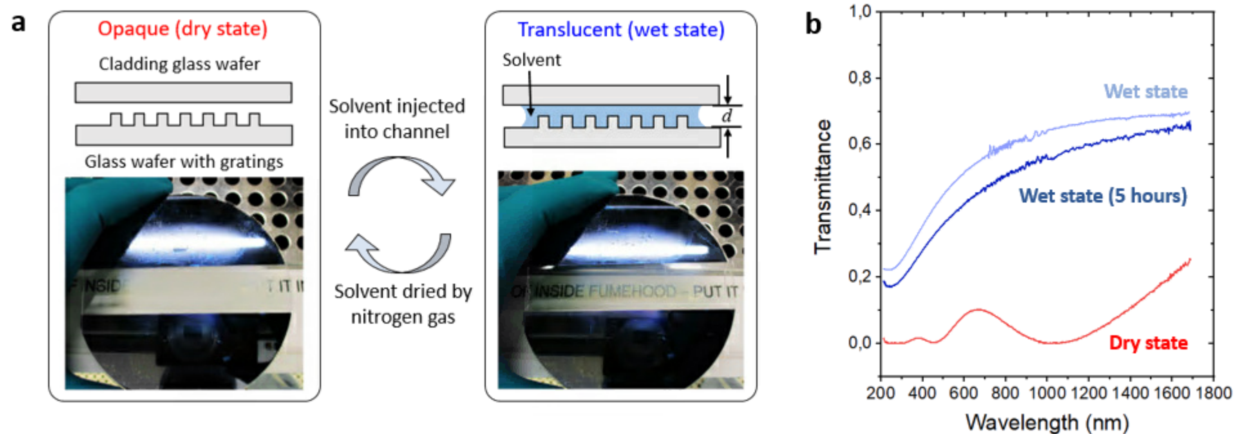

Figure 5. A setup for reversible optical transmittance based on quasi-random SiO_2 gratings: (a) illustration of the design, where a cladding glass wafer is bonded onto the glass wafer with quasi-random gratings on surface (distance d = 500 μm), ethanol solutions can be injected or dried conveniently. Optical photographic images showing the reversible transition between optically translucent and opaque states; (b) measured optical transmittances of the fabricated smart window, with comparison between the dry state, the wet state and the wet state after 5 hours since the injection of solvents.

CONCLUSION

In conclusion, a novel fabrication strategy has been developed in this work for high-throughput wrinkle patterning. To summarize the advantages of this technique compared with conventional fabrication methods: (1) all the materials and equipment are CMOS-compatible in semiconductor industries, making the process easy to be integrated with standard device fabrications; (2) the skin layer generation and the introduction of thermal stress happen simultaneously during the plasma treatment, thus wrinkles can be patterned within few seconds by a single equipment; (3) the patterned wrinkles have a good uniformity in morphology across the whole wafer, thus is favorable for large-scale productions. With the superiorities mentioned above, we hope this technique can

benefit the study and practical applications of wrinkle engineering. Based on the wrinkled resist patterns, quasi-random SiO_2 gratings have been fabricated and exhibit broad-band tunable optical transmittances, enabling smart window applications, more applications for electronic devices will also be interesting to be investigated in the future.

METHODS

Generation of wafer-scale wrinkles: Photoresists were coated onto 4-inch wafers with an automatic spin coater (SUSS MicroTec Lithography GmbH). Without post-baking or developing, the resist-coated wafers were processed inside an inductively coupled plasma etcher (advanced oxide etcher, SPTS Technologies Ltd.). The coil power was set at 1300 W for plasma generations, with pressure of 20 mTorr and chiller temperature at 5 °C. Sulfur hexafluoride (SF_6) gas flow rate was 20 sccm with 160 sccm of helium (He) for plasma stabilization. The sample temperature was estimated to be around 200 °C, which was measured by an irreversible temperature indicator (Thermax). For the demonstration of wrinkles on metal films, a thermal evaporator (Kurt J. Lesker Company Ltd.) was used to deposit aluminum films with various thicknesses.

Fabrication of SiO_2 quasi-random gratings: 4-inch fused silica wafers were chosen as the substrate, the wafers were double-side polished with a thickness of 500 μm. After wrinkles were patterned on the resist layer, the sample was etched with a continuous process inside the same plasma etcher. The coil power and the platen power were set at 2000 W and 200 W respectively, with a gas combination of perfluorocyclobutane (C_4F_8) and He. The resist residues were cleaned by an oxygen plasma in the end of the process.

Characterizations: The surface morphology of wrinkles were characterized by an atomic force microscope (AFM ICON PT, Bruker Co.). Optical microscopic images were captured with a

bright-field microscope (Nikon Eclipse L200). The optical transmittance was measured by a spectroscopic ellipsometer (ellipsometer VASE, J. A. Woolam Co.), where the incoming light is perpendicular to the wafer surface, giving a round probing area with a diameter of around 2 mm.

ASSOCIATED CONTENT

Supporting Information.

The following files are available free of charge.

Optical properties of the photoresists being used, SEM images of wrinkled photoresist surfaces, optical microscopic images of wrinkled Al film on photoresist surfaces, photographic image of a fused silica wafer with random gratings on the surface. (pdf)

AUTHOR INFORMATION

Corresponding Author

*Bingdong Chang bincha@dtu.dk

ACKNOWLEDGMENT

The author would like to thank the DTU Nanolab for instrument support. This work was supported by a research grant (00027987) from VILLUM FONDEN. D. Z. acknowledges the support from the China Postdoctoral Science Foundation (2020M671810, 2020T130602)

REFERENCES

1. Chan, E. P., Smith, E. J., Hayward, R. C., Crosby, A. J. Surface wrinkles for smart adhesion. *Adv. Mater.* **2008**, *20*, 711.

2. Rand, C. J., Crosby, A. J. Friction of soft elastomeric wrinkled surfaces. *J. Appl. Phys.* **2009**, *106*, 064913.

3. Kim, J. B., Kim, P., Pégard, N. C., Oh, S. J., Kagan, C. R., Fleischer, J. W., Stone, H. A., Loo, Y. L. Wrinkles and deep folds as photonic structures in photovoltaics. *Nat. Photonics* **2012**, *6*, 327.

4. Chan, E. P., Crosby, A. J. Fabricating microlens arrays by surface wrinkling. *Adv. Mater.* **2006**, *18*, 3238.

5. Lipomi, D. J., Tee, B. C. K., Vosgueritchian, M., Bao, Z. Stretchable organic solar cells. *Adv. Mater.* **2011**, *23*, 1771.

6. Ohzono, T., Suzuki, K., Yamaguchi, T., Fukuda, N. Tunable optical diffuser based on deformable wrinkles. *Adv. Opt. Mater.* **2013**, *1*, 374.

7. Wu, K., Sun, Y., Yuan, H., Zhang, J., Liu, G., Sun, J. Harnessing Dynamic Wrinkling Surfaces for Smart Displays. *Nano Lett.* **2020**, *20*, 4129.

8. Li, Z., Zhai, Y., Wang, Y., Wendland, G. M., Yin, X., Xiao, J. Harnessing surface wrinkling–cracking patterns for tunable optical transmittance. *Adv. Opt. Mater*. 2017, *5*, 1700425.

9. Cerda, E., Mahadevan, L. Geometry and physics of wrinkling. *Phys. Rev. Lett*. **2003**, 90, 074302.

10. Genzer, J., Groenewold, J. Soft matter with hard skin: From skin wrinkles to templating and material characterization. *Soft Matter* **2006**, *2*, 310.

11. Li, F., Hou, H., Yin, J., Jiang, X. Near-infrared light–responsive dynamic wrinkle patterns. *Sci. Adv*. **2018**, *4*, eaar5762.

12. Choi, W. M., Song, J., Khang, D. Y., Jiang, H., Huang, Y. Y., Rogers, J. A. Biaxially stretchable "wavy" silicon nanomembranes. *Nano Lett.* **2007**, *7*, 1655.

13. Chung, J. Y., Nolte, A. J., Stafford, C. M. Diffusion ‐ controlled, self ‐ organized growth of symmetric wrinkling patterns. *Adv. Mater.* **2009**, *21*, 1358.

14. Kim, H. S., Crosby, A. J. Solvent ‐ responsive surface via wrinkling instability. *Adv. Mater.* **2011**, *23*, 4188.

15. Huntington, M. D., Engel, C. J., Hryn, A. J., Odom, T. W. Polymer nanowrinkles with continuously tunable wavelengths. *ACS Appl. Mater. Interfaces* **2013**, *5*, 6438.

16. Huntington, M. D., Engel, C. J., Odom, T. W. Controlling the orientation of nanowrinkles and nanofolds by patterning strain in a thin skin layer on a polymer substrate. *Angew. Chem*. **2014**, *126*, 8255.

17. Schiltz, A., Paniez, P. J. In-situ determination of photoresist glass transition temperature by wafer curvature measurement techniques. *Microelectron. Eng*. **1995**, *27*, 413.

18. Hussla, I., Enke, K., Grunwald, H., Lorenz, G., Stoll, H. In situ silicon-wafer temperature measurements during RF argon-ion plasma etching via fluoroptic thermometry. *J. Phys. D: Appl. Phys* **1987**, *20*, 889.

19. Lock, E. H., Petrovykh, D. Y., Mack, P., Carney, T., White, R. G., Walton, S. G., & Fernsler, R. F. Surface composition, chemistry, and structure of polystyrene modified by electron-beam-generated plasma. Langmuir **2010**, *26*, 8857.

20. Bruce, R. L., Weilnboeck, F., Lin, T., Phaneuf, R. J., Oehrlein, G. S., Long, B. K., ... Graves, D. B. Relationship between nanoscale roughness and ion-damaged layer in argon plasma exposed polystyrene films. *J. Appl. Phys.* **2010**, *107*, 084310.

21. Chang, B. *PhD thesis*, Technology Development of 3D Silicon Plasma Etching Processes for Novel Devices and Applications, Technical University of Denmark, **2018**.

22. Chang, B., Leussink, P., Jensen, F., Hübner, J., Jansen, H. DREM: Infinite etch selectivity and optimized scallop size distribution with conventional photoresists in an adapted multiplexed Bosch DRIE process. *Microelectron. Eng*., **2018**, *191*, 77.

23. Malitson, I. H. Interspecimen comparison of the refractive index of fused silica. *JOSA* **1965**, *55*, 1205.

24. Kedenburg, S., Vieweg, M., Gissibl, T., Giessen, H. Linear refractive index and absorption measurements of nonlinear optical liquids in the visible and near-infrared spectral region. *Opt. Mater. Express* **2012**, *2*, 1588.

25. Vazquez, G., Alvarez, E., Navaza, J. M. Surface tension of alcohol water+ water from 20 to 50. degree. C. *J. Chem. Eng. Data* **1995**, *40*, 611.